Respiratory Research

RESEARCH

Open Access

Effect of prone position on ventilation-perfusion matching in patients with moderate to severe ARDS with different clinical phenotypes

Shuhe Yang[1†], Qin Sun[1†], Xueyan Yuan[1], Jinlong Wang[1], Haofei Wang[1], Wenhan Hu[1], Qingyun Peng[1], Chen Zhang[1], Xiangquan Li[1], Wei Huang[1], Jianfeng Xie[1], Fengmei Guo[1], Ling Liu[1], Yi Yang[1] and Yingzi Huang[1*]

Abstract

Background ARDS is a heterogeneous syndrome involving different subphenotypes with different clinical features and different responses to treatment strategies. The prone position (PP) is an effective treatment for ARDS; however, whether the effects of prone positioning vary among ARDS patients with different subphenotypes remains unknown.

Objectives To evaluated the impact of PP on ventilation-perfusion matching(VQ matching) by contrast-enhanced Electrical impedance tomography (EIT) in ARDS patients with different subphenotypes.

Methods This was a prospective, observational study at the medical ICU of Zhongda Hospital, Southeast University. ARDS patients undergoing mechanical ventilation were screened and allocated to different subphenotypes based on lung morphology (focal/non-focal) and D-dimer level (low/high D-dimer). EIT was used in the supine position and 3 h, 6 h, and 12 h after the PP during the first PP session.

Results From July 1, 2021, to July 1, 2022, 25 patients were included in this study. 10 patients (40%) were focal ARDS, and 15 were non-focal ARDS based on baseline morphology. 12 patients (48%) were high D-dimer ARDS, and 13 were low D-dimer ARDS based on baseline D-dimer levels. PaO2/FiO2 increased significantly 3 h after prone positioning in focal ARDS patients (130.30[109.94–147.30] vs. 213.50[176.00-256.50] mmHg, $p < 0.001$), while the effect of improved oxygenation was not apparent until 6 h after prone positioning in non-focal ARDS patients (104.60[95.20–127.00] vs. 190.20[160.10-213.20] mm Hg, $p < 0.001$). VQ matching improved after 3 h in the prone position in the focal ARDS group (69.93 ± 6.69 vs. 78.22 ± 5.07, $p = 0.006$) but improved after only 6 h in the prone position in the non-focal ARDS group (67.32 ± 4.78 vs. 78.70 ± 5.93, $p < 0.001$). In ARDS patients with varying levels of D-dimer, increased PaO2/FiO2 (126.60[99.30-146.20] vs. 185.20[112.10–236.00] mmHg, $p = 0.013$) and improved VQ matching (67.60 ± 4.60 vs. 72.97 ± 6.48, $p = 0.023$) were observed at 3 h in the PP in patients with low D-dimer ARDS. In contrast, increased PaO2/

[†]Shuhe Yang and Qin Sun are first authors.

*Correspondence:
Yingzi Huang
yz_huang@126.com

Full list of author information is available at the end of the article

© The Author(s) 2025. **Open Access** This article is licensed under a Creative Commons Attribution-NonCommercial-NoDerivatives 4.0 International License, which permits any non-commercial use, sharing, distribution and reproduction in any medium or format, as long as you give appropriate credit to the original author(s) and the source, provide a link to the Creative Commons licence, and indicate if you modified the licensed material. You do not have permission under this licence to share adapted material derived from this article or parts of it. The images or other third party material in this article are included in the article's Creative Commons licence, unless indicated otherwise in a credit line to the material. If material is not included in the article's Creative Commons licence and your intended use is not permitted by statutory regulation or exceeds the permitted use, you will need to obtain permission directly from the copyright holder. To view a copy of this licence, visit http://creativecommons.org/licenses/by-nc-nd/4.0/.

FiO2(105.20[95.20-124.10] vs. 195.2[183.20-213.20], $p < 0.001$) and improved VQ matching (67.19 ± 6.70 vs. 72.50 ± 6.37, $p < 0.001$) were revealed only after 6 h in the prone position in high D-dimer ARDS patients.

Conclusions For moderate to severe ARDS patients, non-focal and high D-dimer ARDS patients need longer PP to improve oxygenation and VQmatching than the focal and low D-dimer patients.

Clinical Trial Registration This was a prospective, observational study registered in the Chinese Clinical Trial Registry (ChiCTR2200055442, https://www.chictr.org.cn/), on June 30, 2021.

Keywords Acute respiratory distress syndrome, Prone position, Subphenotype, Ventilation-perfusion matching, Electrical impedance tomography

Background

Acute respiratory distress syndrome (ARDS) is a prevalent condition in the intensive care unit (ICU) characterized by a high mortality rate [1], and prone positioning has been an important treatment modality for improving oxygenation and prognosis in ARDS patients [2].

An inaugural report on prone positioning in ARDS patients surfaced in 1976 [3], detailing noteworthy enhancements in oxygenation upon transitioning patients from the supine to the prone position. The prone position may induce a spectrum of physiological effects, including the alleviation of lung pressure, diminishment of areas prone to collapse, enhancement of lung function, rectification of gas exchange imbalance through more uniform blood and airflow redistribution, reduction of ventilator reliance, and facilitation of improved clearance of secretions generated during lung diseases. In the last decade, conclusive evidence supporting the mortality reduction attributed to prone positioning in severe ARDS patients has emerged [4–6]. Nonetheless, recent studies have cast doubt on the efficacy of prone positioning since it can cause heightened lung hyperinflation in ARDS patients [7]. This suggests that individual differences may exist in the response of ARDS patients to prone positioning therapy.

ARDS is a markedly heterogeneous syndrome, leading to varied responses among patients to different treatments. Classifying ARDS patients into subphenotypes is a good perspective for explaining the different clinical characteristics of ARDS patients and their varying responses to treatment and imaging features, and biomakers are the most commonly used indicators for identifying ARDS subphenotypes [8–12]. Within the LIVE trial, mortality reduction was observed at 90 days when personalized positive end-expiratory pressure (PEEP) and prone positioning strategies were employed, guided by clinical phenotypes (focal versus non-focal), specifically among patients treated with each regimen [4, 13]. Secondary analyses of the LUNG-SAFE study [14] and the ALVEOLI trial [12] both indicated potential benefits for patients with hyperinflammation when employing high PEEP, in contrast to the hypoinflammatory subphenotype. This finding implies that inflammation levels may influence the uniformity of lung ventilation. Similarly, ARDS patients exhibiting diverse imaging features and inflammation levels may manifest distinct responses to prone positioning. In contrast to patients with non-focal ARDS, those with focal ARDS exhibit more pronounced dorsal lung collapse and may demonstrate greater responsiveness to prone positioning. Nevertheless, pertinent studies investigating the response of patients with distinct ARDS phenotypes to prone position treatment are currently lacking.

In this study, we aimed to compare the impact of PP on ventilation and pulmonary perfusion between moderate-to-severe ARDS patients with different subphenotypes using contrast-enhanced electrical impedance tomography (EIT) to determine the relationship between ARDS subphenotypes and patient response to PP.

Method

The study was conducted in the medical ICU (Zhongda Hospital of Southeast University, Nanjing, China). The research had been performed in accordance with the Declaration of Helsinki and approved by the Institutional Review Board of Zhongda Hospital (No. 2021ZDSYLL171-P01). Informed consent was obtained by local regulations. This was a prospective, observational study registered in the Chinese Clinical Trial Registry (ChiCTR2200055442).

Study population

Consecutive adult patients admitted to our ICU between July 1, 2021, and July 1, 2022, underwent screening. The inclusion criteria were (1) invasive ventilation; (2) moderate to severe ARDS, as per the Berlin definition before the study [15]; and (3) availability of physiological data before and after prone training. The exclusion criteria included refusal to participate, contraindications to EIT (e.g., chest deformity, unstable spinal injury or fracture, open chest wound, pacemaker implantation), and use of extracorporeal membrane oxygenation.

Study protocol

The patient underwent deep sedation, paralysis, and mechanical ventilation in synchronized intermittent

mandatory ventilation (SIMV) mode. Throughout all study measurements, ventilator settings were standardized for all patients, including a tidal volume (Vt) of 6–8 mL/kg of predicted body weight and the respiratory rate adjusted to maintain a pH between 7.35 and 7.45. The PEEP was set according to the low FiO2-PEEP table of the ARDSnet to maintain the following oxygenation goals: SpO2 between 88 and 95%, and PaO2 between 55 and 80 mmHg in the supine position [16]. The PEEP periods remained unchanged in the prone position. Arterial blood gas (ABG) analysis, ventilator parameters, EIT monitoring, and hemodynamic monitoring were conducted in the following positions: supine position (SP), prone position at 3 h (PP_{3h}), prone position at 6 h (PP_{6h}), and prone position at 12 h (PP_{12h}). The ABG recording data included pH, carbon dioxide partial pressure, bicarbonate ion concentration, oxygenation index, and other relevant parameters. The ventilator parameters included PEEP, respiratory frequency, airway peak pressure, plateau pressure, respiratory system compliance, and other relevant measures. EIT monitoring data comprised changes in overall and local impedance values, with offline analysis of the data. Parameters such as the dead space(%), shunt(%), lung ventilation-perfusion matching(VQ matching, %), inhomogeneity index (GI), lung ventilation, and lung perfusion were calculated for each region of interest (ROI). Blood flow kinetic parameters included heart rate (HR), central venous pressure (CVP), and mean arterial pressure (MAP).

EIT data

EIT tape containing 16 electrodes was placed between the fourth or fifth intercostal space on the patient's chest wall and subsequently connected to an EIT monitor (PulmoVista 500; Dräger Medical GmbH, Lübeck, Germany). The EIT signals were acquired at a frequency of 50 Hz. After a 5-minute baseline recording of the EIT data, we performed end-expiratory breath-holds lasting 15 s. A typical first-pass kinetic impedance dilution curve was generated by injecting 10 ml of 5% NaCl solution through the internal jugular vein for 2 s. Ventilation images of the EIT were obtained by offline analysis of the impedance averages over 2 consecutive minutes. The lung region was divided equally into 4 ROIs based on the vertical distance from the ventral region to the dorsal region. These regions were labeled ROI1, ROI2, ROI3, and ROI4 from the ventral region to the dorsal region respectively. By analyzing the images acutely, we obtained and calculated the following ventilation-related parameters [17]:

1) The lung ventilation region, which was defined as pixels with a tidal change ≥ 20% of the maximum pixel impedance change;.
2) Percentage of the overall lung ventilation region for each ROI of the lung ventilation region;.
3) The GI was defined as the sum of the absolute values of the difference between the median respiratory impedance change and each pixel value, as a percentage of the total impedance value [18].

The lung perfusion maps were obtained based on the change in impedance drop after injection of sodium chloride solution during end-expiratory occlusion. By analyzing the images, we calculated the following perfusion-related parameters [19]:

1) The lung perfusion region, which was defined as pixels with values ≥ 20% of the maximum pixel value in the perfusion map.
2) Percentage of the overall lung perfusion region for each ROI of the lung perfusion region;

By amalgamating the pixel-level data pertaining to lung ventilation and perfusion (Fig. 1), we obtained the following results:

1) The percentage of the shunt region was calculated as the ratio of all pixels demonstrating perfusion without concomitant ventilation to the total number of pixels categorized as either ventilation or perfusion.
2) The percentage of the dead space region was calculated as the ratio of all pixels demonstrating ventilation without concomitant perfusion to the total number of pixels categorized as either ventilation or perfusion.
3) The percentage of ventilation-perfusion matched regions was calculated as the number of pixels that were both ventilated and perfused divided by the total number of pixels that were ventilated and/or perfused.

Physiological effects of the prone position on pulmonary ventilation and perfusion in a patient with typical focal ARDS. EIT monitoring is shown in Fig. 1.

Identification of subphenotypes

Lung CT scans were obtained 24 h before all patients were placed in the prone position. All lung CT scans were performed with patients in the supine position. According to the Fleischner Society Nomenclature Committee, CT attenuation is classified into consolidation and ground-glass opacities [20]. Consolidation is defined as a uniform increase in lung parenchymal attenuation, resulting in the loss of definition of the margins of both the blood vessels and airway walls. Ground-glass opacity, on the other hand, is characterized by a diffuse haziness

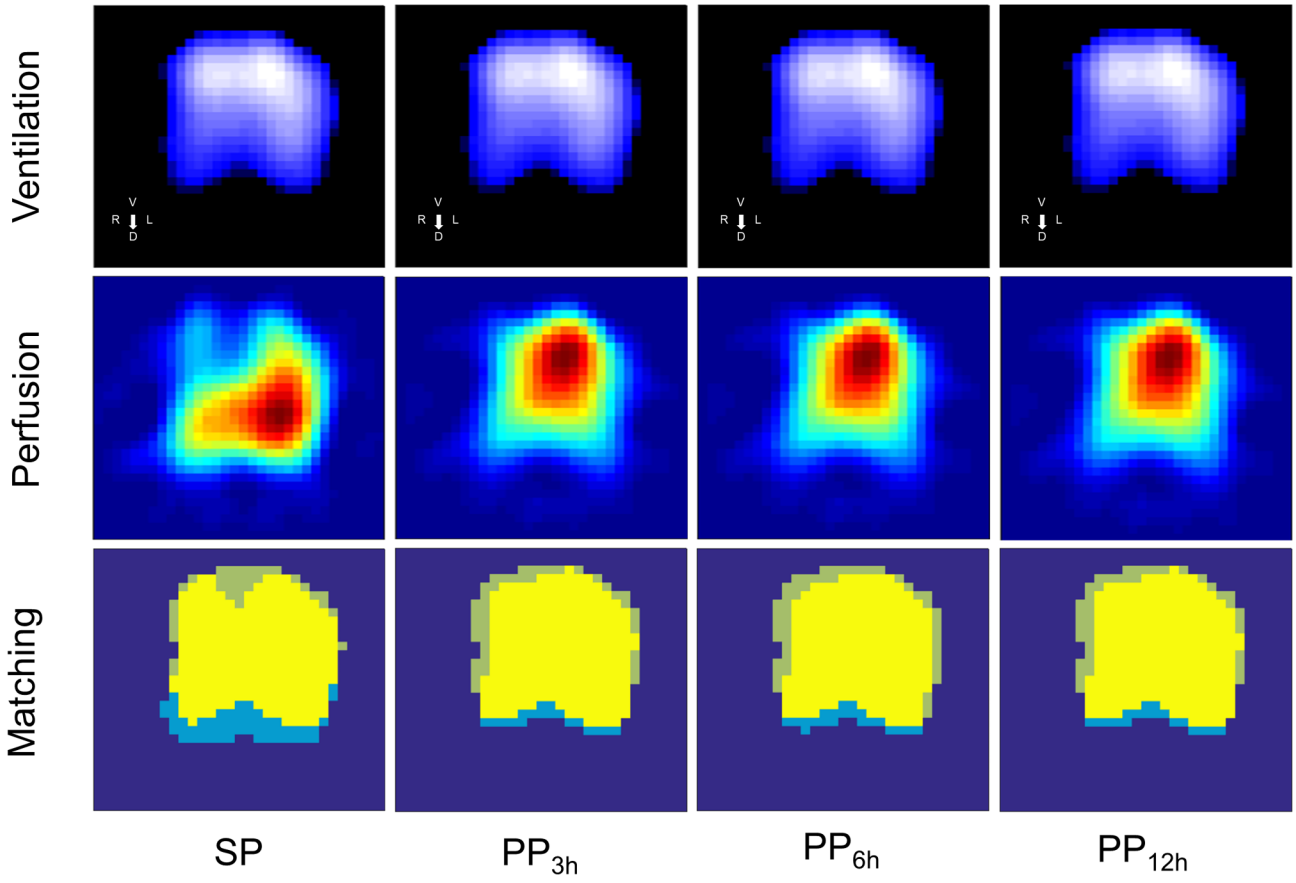

Fig. 1 Effect of prone position on ventilation/perfusion matching (VQ matching) in a patient with typical focal ARDS. From top to bottom, there was lung ventilation (blue-white gradient area), perfusion (red-yellow area), and ventilator-perfusion matching. From doing to right, they were supine (SP), prone for 3 h (PP_{3h}), prone for 6 h (PP_{6h}), and prone for 12 h (PP_{12h}). The ventilation area is defined as the pixel point where the impedance change is greater than 20% of the maximum tidal impedance change in the functional ventilation image. The perfusion area is defined as a pixel that is greater than 20% of the maximum dose-dependent impedance change in the functional perfusion image. High-ventilation and low-perfusion areas are marked in blue (for dead space), low-ventilation and high-perfusion areas are marked in red (for shunt), and areas with good ventilation-perfusion matching are marked in bright yellow (for VQ matching)

of the lung parenchyma with increased density, yet preserving the contours of the bronchi and blood vessels. Both patterns may be associated with bronchial wall thickening. For the classification of ARDS, the distribution of lung attenuation is critical. If consolidation shows a lobar or segmental pattern, and is localized to the lower or posterior regions of the lung, the patient is classified as having focal ARDS. In contrast, if attenuation is diffusely distributed throughout the lung or extends beyond the interlobar fissures, accompanied by widespread or segmental loss of ventilation, the patient is classified as having non-focal ARDS [8, 11, 14]. Two intensivists independently and blindly reviewed and classified the patients based on the location of lung lesions. In cases where there was a discrepancy between their classifications, a senior radiologist was consulted to make the final determination (Additional file 1: Figure S1;).

D-dimer serves as both a marker of coagulation activation and a potential indicator of inflammatory activation [12, 21]., all patients were categorized into high D-dimer and low D-dimer subphenotypes according to the median D-dimer levels detected in the peripheral blood 24 h before prone positioning.

Statistical analysis

The sample size was similar to that in previous physiological studies [22, 23]. Statistical analysis was performed using SPSS 27.0 (SPSS Inc., Chicago, IL) and Prism 8.0.1 (GraphPad Software, San Diego, CA, USA). The normality of all continuous variables was assessed using the Shapiro–Wilk test. Normally distributed date are presented as the mean ± SD; otherwise, the median and interquartile range are reported. To assess the impact of time points on the variables, Mauchly's test was conducted for sphericity and repeated-measures ANOVA was employed with post hoc Bonferroni correction for multiple comparisons. In cases of sphericity violation (i.e., Mauchly's test p-value < 0.05), the Greenhouse–Geisser method was

applied for correction. The Pearson regression coefficient was utilized to evaluate the correlation between continuous variables. All the statistical tests were two-tailed, and a significance level of $p < 0.05$ was considered to indicate statistical significance.

Results

Patient characteristics

Twenty-five patients who were diagnosed with moderate to severe ARDS, and who received mechanical ventilation in the ICU of Zhongda Hospital of Southeast University between July 2020 and July 2021 were included. Among them, 18 (72%) were male, with an average age of 66.56 ± 11.72 years. The average APACHE II score within the initial 24 h of admission was 20.88 ± 7.22, and the average SOFA score was 10.92 ± 2.77. Severe ARDS was present in 11 (44%) of the patients. The patients' PaO2/FiO2 before enrollment averaged 120.38 ± 24.56 mm Hg. The arterial blood carbon dioxide partial pressure was 39.17 ± 7.88 mm Hg. The Vt was 6.21 ± 0.96 ml/kg predicted body weight (PBW), the PEEP was 10.00(8.00–12.00) cmH2O, the plateau pressure was 21.71 ± 4.07 cmH2O, the driving pressure was 11.31 ± 2.49 cmH2O, and the static compliance of the respiratory system was 36.48 ± 10.87 ml/cmH2O. More detailed clinical characteristics of the study population are presented in Table S1 of additional file 1.

Lung morphology subphenotypes

Subphenotyping was conducted based on the lung morphological characteristics of patients before enrollment. Ten patients (40%) were classified as having focal ARDS, while the other patients exhibited non-focal ARDS. No significant differences in sex, age, BMI, APACHE II score, or SOFA score were observed between the two groups before enrollment. Ventilation-perfusion matching at the SP in the non-focal ARDS group was significantly lower than that in the focal group (67.28 ± 8.78% vs. 52.25 ± 15.62%, $p = 0.011$). The PaO2/FiO2 ratio at the SP in patients with non-focal ARDS was significantly lower than that in patients with focal ARDS (130.30[109.94–147.30] vs. 104.60[95.20–127.00] mm Hg, $p = 0.024$). No significant differences in the proportion of dead space, shunt proportion, or hemodynamic parameters were observed between the two groups of patients at the SP (Table 1).

Focal ARDS patients exhibit a more rapid improvement in oxygenation after assuming the prone position. Compared with that in the SP group, oxygenation significantly increased after 3 h in the prone position (130.30[109.94–147.30] vs. 213.50[176.00-256.50] mm Hg, $p < 0.001$) in the focal ARDS group, while oxygenation increased until 6 h after PP in non-focal ARDS group (104.60[95.20–127.00] vs. 190.20[160.10-213.20] mm Hg, $p < 0.001$). The improvement in oxygenation was sustained for 12 h after PP in both groups.

Comparable findings were noted for ventilator-perfusion matching under EIT monitoring. In comparison with SP, there was a notable increase in ventilator perfusion after 3 h in the prone position (69.93 ± 6.69 vs. 78.22 ± 5.07, $p = 0.006$). In patients with non-focal ARDS, ventilator-perfusion matching at PP_{3h} did not significantly increase compared with that at SP, whereas significant increases were observed at PP_{6h} and PP_{12h} (Fig. 1). In focal ARDS patients, the shunt significantly decreased at PP_{3h} compared with that at SP (17.37 ± 5.38 vs. 12.80 ± 3.80, $p = 0.042$), while the dead space did not change significantly (12.70 ± 4.11 vs. 8.98 ± 3.03, $p = 0.056$). For non-focal ARDS patients, the PP_{6h} shunt was significantly reduced (16.72 ± 5.25 vs. 14.01 ± 4.34, $p = 0.023$), and the dead space also decreased significantly (15.93 ± 3.21 vs. 12.27 ± 3.72, $p = 0.007$) (Fig. 2).

In focal ARDS patients, the prone position primarily affected lung ventilation in ROI 2 and ROI 4. In ROI 2, the proportion of patients with lung ventilation at PP_{3h}, PP_{6h}, and PP_{12h} significantly decreased compared with that at SP, while in ROI4, the proportion of patients with lung ventilation at PP_{3h}, PP_{6h}, and PP_{12h} significantly increased compared with that at SP (Additional file 1: Figure S2; Table S2). The prone position had no significant effect on pulmonary perfusion in focal ARDS patients. In non-focal ARDS patients, as the prone position continued, the proportion of patients with lung ventilation in ROI1 and ROI2 decreased, while the proportion of patients with lung ventilation in ROI3 and ROI4 increased. Compared with those in the SP, at PP_{6h}, the proportion of pulmonary perfusion in ROI2 decreased, and the proportion of pulmonary perfusion in ROI3 increased (Additional file 1: Figure S2; Table S3).

D-dimer phenotypes

The median D-dimer level among all patients was 1563 μg/L. D-dimer subphenotypes were categorized based on baseline D-dimer levels, with 13 patients classified into the low D-dimer ARDS group and 12 patients classified into the high D-dimer ARDS group. There was no significant difference in sex, age, BMI, disease duration, APACHE II score, SOFA score, or 28-day mortality between the two groups before enrollment. The baseline C-reactive protein levels in patiens with high D-dimer ARDS were significantly greater than those in patients with low D-dimer ARDS (190.2 ± 93.1 vs. 75.6 ± 57.6, $p = 0.001$). The baseline dead space in the high D-dimer ARDS group was significantly greater than that in the low D-dimer ARDS group (15.2%±3.8 vs. 14.2 ± 4.0%, $p = 0.025$). No significant difference in baseline shunt or ventilation-perfusion matching was observed between the two groups of patients (Table 2).

Table 1 Main characteristics at admission for different morphology subphenotype ARDS

Characteristics	Focal ARDS, $n=10$	Non-focal ARDS, $n=15$	*p*-value
Age, yr	70.40 ± 12.85	64.00 ± 10.55	0.186
Male, n (%)	9(90)	9(60)	0.102
Body mass index, kg/m^2	23.92 ± 3.17	25.01 ± 3.42	0.429
APACHE II score at ICU admission	18.70 ± 6.93	22.33 ± 7.27	0.225
SOFA score at ICU admission	10.80 ± 2.53	11.00 ± 3.00	0.864
Arterial blood gases			
pH	7.39 ± 0.07	7.39 ± 0.09	0.969
PaO_2/FiO_2	130.30(109.94–147.30)	104.60(95.20–127.00)	0.024
$PaCO_2$	38.08 ± 7.70	39.89 ± 8.17	0.584
Respiratory parameters			
Respiratory rate, breaths/min	18.6 ± 4.17	20.67 ± 2.44	0.131
Positive end-expiratory pressure, cmH_2O	9.00(8.00-10.50)	10.00(10.00–12.00)	0.158
Respiratory system compliance, ml/cmH_2O	41.02 ± 13.12	33.45 ± 8.22	0.088
Peak pressure, cmH_2O	25.87 ± 3.42	21.02 ± 5.05	0.089
Plateau pressure, cmH_2O	19.78 ± 3.16	23.00 ± 4.18	0.049
Driving pressure, cmH_2O	10.17 ± 2.47	12.07 ± 2.27	0.060
Mechanical power, J/min	14.69 ± 3.85	17.90 ± 3.37	0.038
Hemodynamic parameters			
Central venous pressure, mmHg	11.00(4.00-11.25)	12.00(9.00–14.00)	0.424
Mean arterial pressure, mmHg	77.60 ± 3.84	79.58 ± 14.26	0.674
Heart rate, beats per minute	101.00(83.50–108.00)	84.00(66.00–91.00)	0.167
Cardiac output, l/min	4.79(4.35–8.84) *	5.06(4.30–4.50) †	0.340
Electrical impedance tomography			
ROI 1 of ventilation distribution, %	15.62(7.54–19.97)	12.43(11.14–15.26)	0.479
ROI 2 of ventilation distribution, %	47.79 ± 6.93	49.23 ± 5.58	0.570
ROI 3 of ventilation distribution, %	33.15 ± 12.30	32.69 ± 4.55	0.895
ROI 4 of ventilation distribution, %	4.85 ± 3.06	579 ± 2.91	0.446
ROI 1 of perfusion distribution, %	11.99 ± 4.60	10.44 ± 5.23	0.458
ROI 2 of perfusion distribution, %	47.61 ± 5.78	46.86 ± 5.66	0.751
ROI 3 of perfusion distribution, %	34.4 ± 6.82	34.46 ± 7.50	0.724
ROI 4 of perfusion distribution, %	6.00 ± 2.77	7.24 ± 2.36	0.244
GI index-ventilation	0.40 ± 0.05	0.39 ± 0.05	0.621
Shunt, %	15.08 ± 7.56	16.01 ± 14.79	0.857
Dead space, %	17.63 ± 12.32	31.86 ± 19.83	0.056
VQ matching, %	67.28 ± 8.78	52.25 ± 15.62	0.011
Inflammation parameters			
White blood cell count, per microliter	12.75(8.65–19.53)	9.11(5.58–14.68)	0.067
Neutrophils/lymphocytes	20.42(11.11–50.81)	11.71(7.42–30.81)	0.258
D-dimer, ug/L	1452.50(902.50–3177.00)	3426.00(598.00-7326.00)	0.189
C-reactive protein, mg/L	150.66 ± 100.81	117.29 ± 92.20	0.402
Procalcitonin, ng/ml	6.24(2.36–28.70)	1.24(0.30–2.31)	0.100
D-dimer subphenotype			
High D-dimer subphenotype, n(%)	4(40)	8(53.3)	0.806

APACHE, acute physiology, and chronic health evaluation; SOFA, sequential organ failure assessment; ROI, region of interest; ARDS, acute respiratory distress syndrome; Values are represented as count (percentage), mean ± standard deviation, or median (interquartile range)

p-value indicates Mann–Whitney U test and Pearson χ^2 test between change in value between focal ARDS and non-focal ARDS

**, data were unavailable for 2 patients;†, data were unavailable for 4 patients*

The low D-dimer phenotype of ARDS patients exhibited a more rapid improvement in the oxygenation index after assuming the prone position. For patients with low D-dimer ARDS, oxygenation significantly increased after 3 h in the prone position compared with that in the SP position (126.60[99.30-146.20] vs. 185.20[112.10–236.00] mm Hg, $p=0.013$). For patients with high D-dimer ARDS, oxygenation increased significantly at PP_{6h}(105.20[95.20-124.10] vs. 131.30[99.00-163.30] mm Hg, $p<0.001$). Compared with that in the

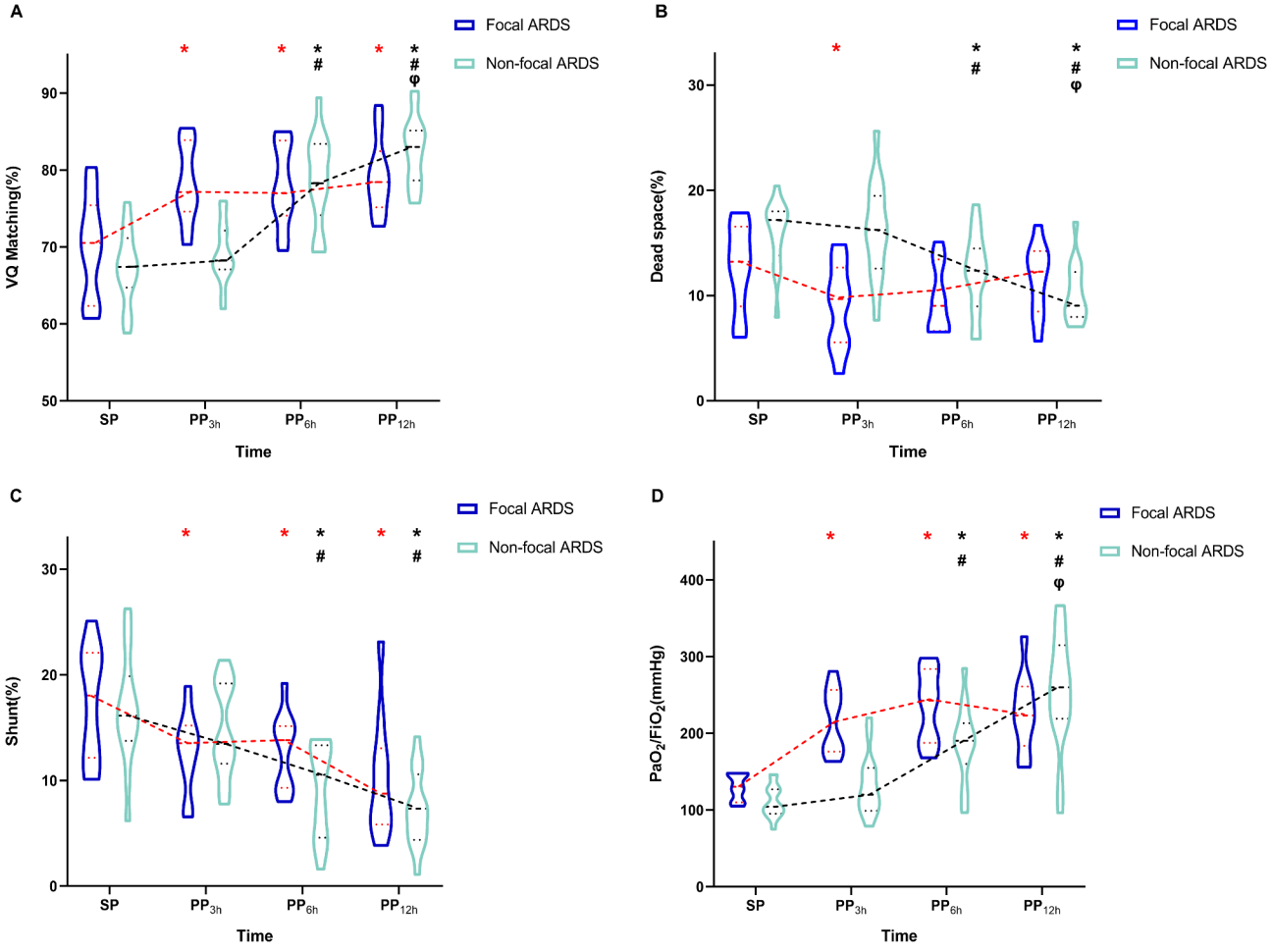

Fig. 2 Effects of prone position on the VQ matching, dead space, shunt, and oxygenation in patients with different morphological subphenotypes of ARDS. (**A**) The effect of prone position on VQ matching of different morphological subphenotypes of ARDS; (**B**) The effect of prone position on the dead space of different morphological subphenotypes of ARDS; (**C**) The effect of prone position on the shunt of different morphological subphenotypes of ARDS; (**D**) Effect of prone position on oxygenation in different morphological subphenotypes of ARDS; blue: focal ARDS; light green: non-focal ARDS; red dotted line: change trend of focal ARDS; black dotted line: non-focal ARDS change trend of sexual ARDS; SP: supine position; PP_{3h}: prone position for 3 h; PP_{6h}: prone position for 6 h; PP_{12h}: prone position for 12 h.*vs. SP,$p < 0.05$;$^{\#}$vs. PP_{3h}, $p < 0.05$;$^{\varphi}$vs. PP_{6h}, $p < 0.05$

SP group, the degree of ventilation-perfusion matching in the low D-dimer ARDS group was significantly greater at PP_{3h} (67.60 ± 4.60 vs. 72.97 ± 6.48, $p = 0.0023$). In patients with low D-dimer ARDS, the amount of dead space did not change at PP_{3h}(14.15 ± 4.00 vs. 12.94 ± 6.43, $p = 0.57$), whereas the amount of shunt decreased at PP_{3h}(18.21 ± 3.93 vs. 14.09 ± 3.67, $p = 0.011$). However, for patients with high D-dimer ARDS, the amount of dead space decreased at PP_{12h} (15.16 ± 3.82 vs. 9.12 ± 2.38, $p < 0.001$), while the amount of the shunt decreased significantly at PP_{6h} (15.65 ± 6.20 vs. 8.69 ± 4.28, $p = 0.004$) (Fig. 3).

In patients with the low D-dimer phenotype of ARDS, the proportion of patients with lung ventilation in ROI 1 and ROI 2 gradually decreased, while the proportion of patients with lung ventilation in ROI 3 and ROI 4 increased following prone positioning (Additional file 1: Figure S3; Table S4). A similar phenomenon of lung ventilation was observed in patients with a high D-dimer phenotype of ARDS. In terms of regional lung perfusion, the proportion of lung perfusion in ROI2 significantly decreased, and the proportion of lung perfusion in ROI3 significantly increased at PP_{3h} in patients with the high D-dimer phenotype of ARDS compared with those in the SP group (Additional file 1: Figure S3; Table S5).

Discussion

Concerning the use of EIT, this study has provided some detailed evidence about the effects of PP during mechanical ventilation in ARDS patients with different subphenotypes. The main findings of our study are as follows: (1) Prone positioning rapidly improved oxygenation and ventilation-perfusion matching for focal ARDS patients or low D-dimer ARDS patients and the effects

Table 2 Main characteristics at admission for different inflammation subphenotype ARDS

Characteristics	Low D-dimer, *n* = 13	High D-dimer, *n* = 12	*p*-value
Age, yr	68.2 ± 10.6	64.8 ± 13.1	0.490
Male, n (%)	10(76.9)	8(66.7)	0.568
Body mass index, kg/m^2	24.1 ± 3.1	25.1 ± 3.6	0.469
APACHE II score at ICU admission	21.4 ± 6.2	20.3 ± 8.4	0.724
Sequential organ failure assessment score at ICU admission	11.0 ± 2.6	10.8 ± 3.0	0.884
Arterial blood gases			
pH	7.39 ± 0.09	7.40 ± 0.08	0.777
PaO_2/FiO_2	126.60(99.30-146.20)	105.20(95.20-124.10)	0.571
$PaCO_2$	39.38 ± 8.30	38.94 ± 7.75	0.894
Respiratory parameters			
Respiratory rate, breaths/min	20.00(16.50–22.00)	20.0(20.0-20.8)	0.234
Positive end-expiratory pressure, cmH_2O	11.0 ± 2.4	9.8 ± 2.3	0.192
Respiratory system compliance, ml/cmH_2O	36.44 ± 11.27	36.53 ± 10.93	0.986
Peak pressure, cmH_2O	28.4 ± 4.3	27.2 ± 5.2	0.536
Plateau pressure, cmH_2O	22.6 ± 4.3	20.8 ± 3.7	0.271
Driving pressure, cmH_2O	11.6 ± 2.9	11.0 ± 2.1	0.574
Mechanical power, J/min	16.55 ± 3.67	16.70 ± 4.18	0.930
Hemodynamic parameters			
Central venous pressure, mmHg	10.77 ± 4.64	10.50 ± 3.85	0.877
Mean arterial pressure, mmHg	80.74 ± 10.77	76.67 ± 11.71	0.374
Heart rate, beats per minute	88.00(81.50–105.00)	87.50(70.00-100.25)	0.467
Cardiac output, l/min	4.52(4.30–8.10) *	4.4(4.3–4.5) †	0.374
Electrical impedance tomography			
ROI 1 of ventilation distribution, %	14.5 ± 4.7	11.5 ± 6.3	0.182
ROI 2 of ventilation distribution, %	49.0 ± 7.1	48.3 ± 5.0	0.774
ROI 3 of ventilation distribution, %	32.2 ± 9.5	33.6 ± 7.2	0.679
ROI 4 of ventilation distribution, %	4.3 ± 3.2	6.6 ± 2.1	0.044
ROI 1 of perfusion distribution, %	12.2 ± 5.9	9.8 ± 3.4	0.232
ROI 2 of perfusion distribution, %	42.9(39.5–48.8)	49.76(46.26–51.87)	0.085
ROI 3 of perfusion distribution, %	36.2 ± 9.2	33.8 ± 3.7	0.398
ROI 4 of perfusion distribution, %	6.3 ± 2.9	7.3 ± 2.1	0.332
GI index-ventilation	0.39 ± 0.04	0.39 ± 0.06	0.931
Shunt, %	18.2 ± 3.9	15.7 ± 6.2	0.168
Dead space, %	14.2 ± 4.0	15.2 ± 3.8	0.025
VQ matching, %	67.6 ± 4.6	69.2 ± 6.7	0.133
Inflammation parameters			
White blood cell count, per microliter	12.8(9.1–15.2)	7.5(5.0-13.8)	0.748
Neutrophils / Lymphocytes	21.2(7.1–32.8)	15.9(8.7–37.3)	0.748
D-dimer, ug/L	814.00(498.50-1147.50)	4220.5(3433.5-8540.3)	0.045
C-reactive protein, mg/L	75.6 ± 57.6	190.2 ± 93.1	0.001
Procalcitonin, ng/ml	2.3(0.8–6.2)	1.7(0.5–5.4)	0.454
Morphology subphenotype			
Focal ARDS(n, %)	6(46.2)	4(33.3)	0.806

APACHE, acute physiology, and chronic health evaluation; SOFA, sequential organ failure assessment; ROI, region of interest; ARDS, acute respiratory distress syndrome; Values are represented as count (percentage), mean ± standard deviation, or median (interquartile range)

p-value indicates Mann–Whitney U test and Pearson χ^2 test between change in value between low D-dimer ARDS and high D-dimer ARDS

**, data were unavailable for 2 patients;†, data were unavailable for 4 patients*

were sustained for at least 12 h, whereas patients in the non-focal ARDS group or high D-dimer ARDS group required a minimum of 6 h for significant enhancements in oxygenation and ventilation-perfusion matching. (2) For overall ARDS, prone positioning can reduce shunts, decrease dead space, and increase ventilation-perfusion matching, thereby improving oxygenation. (3) For focal ARDS patients, prone positioning for 3 h may improve oxygenation by reducing shunts and increasing ventilation-perfusion matching; for non-focal ARDS patients,

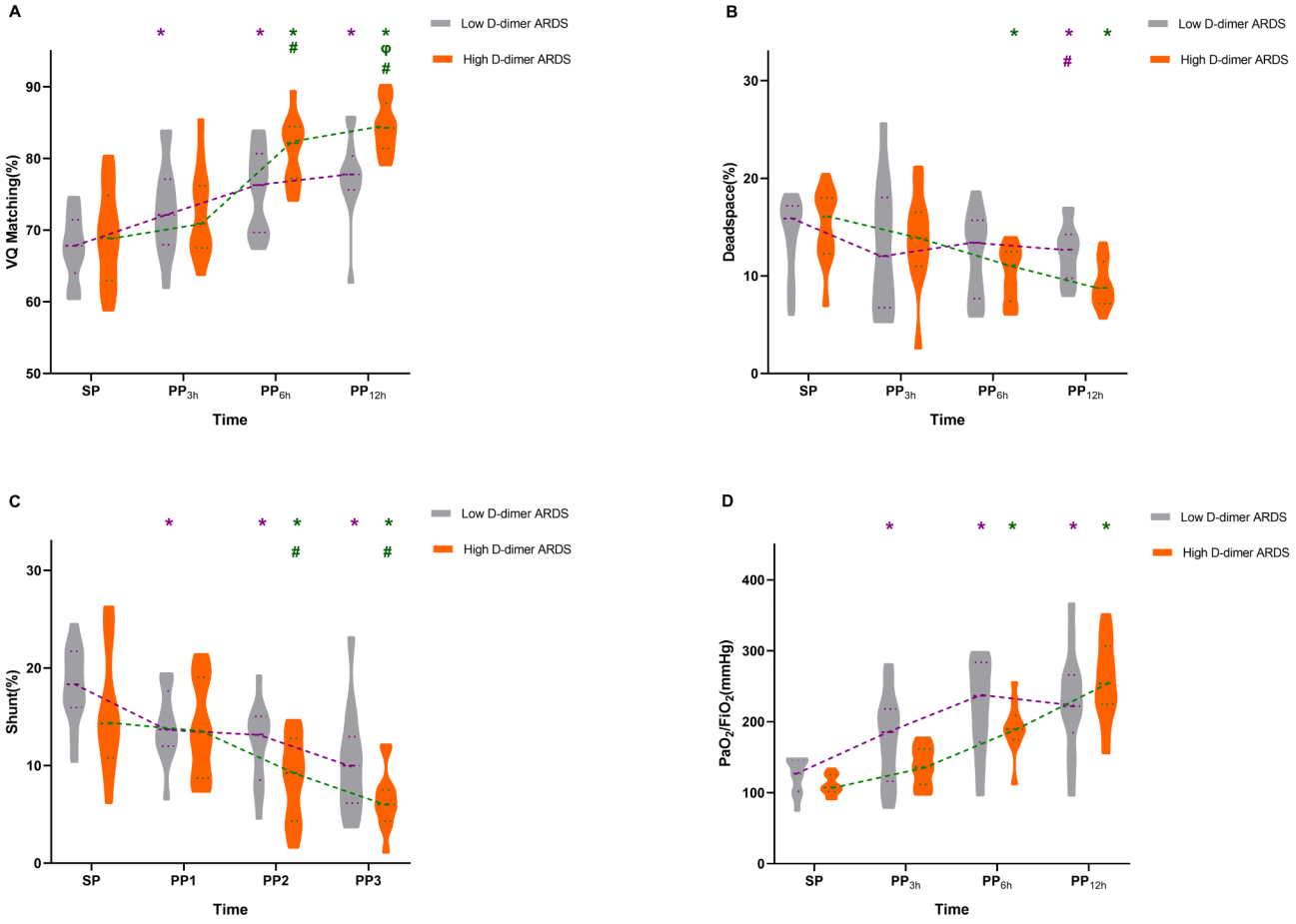

Fig. 3 Effects of prone positioning on the VQ matching, dead space, shunt, and oxygenation in patients with different D-dimer subphenotypes of ARDS. (**A**) The effect of the prone position on the VQ matching of different D-dimer subphenotypes of ARDS; (**B**) the effect of the prone position on the dead space of different D-dimer subphenotypes of ARDS; (**C**) the effect of the prone position on the shunting of different D-dimer subphenotypes of ARDS; (**D**) the effect of the Prone position on oxygenation of different D-dimer subphenotypes of ARDS; Gray: low D-dimer ARDS; Orange: high D-dimer ARDS; Purple dotted line: change trend of low D-dimer ARDS; Green dotted line: change trend of high D-dimer ARDS; SP: supine position; PP_{3h}: prone position for 3 h; PP_{6h}: prone position for 6 h; PP_{12h}: prone position for 12 h.*vs. SP,$p < 0.05$;$^{\#}$vs. PP_{3h}, $p < 0.05$;$^{\varphi}$vs. PP_{6h}, $p < 0.05$

prone positioning for 6 h simultaneously reduces the amount of dead space and shunts, resulting in increased ventilation, perfusion and oxygenation. (4) In patients with low D-dimer ARDS, prone positioning for 3 h can reduce shunts and improve oxygenation; in high D-dimer ARDS, prone positioning for 6 h can reduce dead space and shunts, increase ventilation-perfusion matching, and improve oxygenation.

Prone positioning can alter the redistribution of pulmonary ventilation and pulmonary perfusion. (1) A prone position can promote the redistribution of pulmonary ventilation, as observed in previous studies [22, 24, 25]. (2) The effect of the prone position on pulmonary perfusion is inconsistent. While some studies have indicated no significant impact on pulmonary perfusion [25, 26], recent studies utilizing EIT measurements have shown improved dorsal lung perfusion [22, 27]. This finding aligns with our study and may be influenced by the study population or the method of monitoring lung perfusion. Prone positioning can significantly improve ventilation-perfusion matching, consistent with previous research findings [22, 28–30]. A recent study suggested that prone positioning can improve dorsal shunting and reduce V/Q mismatch in early ARDS, which is consistent with what we have observed in focal ARDS [30].

The varied response of ARDS patients with different imaging phenotypes to prone positioning therapy may be explained by the underlying pathophysiology of ARDS and its influence on lung mechanics and perfusion. Focal ARDS is characterized by increased localized lung damage, frequently leading to dorsal lung hypoventilation. In classic ARDS, poor compliance of the lung, coupled with a four-to fivefold increase in mass, leads to a significant increase in the pleural pressure gradient. This results in severe compressive atelectasis and non-dependence in gravity-dependent lung regions, causing regional overdistension in the lungs [9, 31]. Therefore, in the prone position, these alveoli may open as the superimposed

pressure in the dorsal region is relieved [32]. Prone positioning may optimize ventilation-perfusion matching and enhance oxygenation by redistributing ventilation to affected areas. In focal ARDS, a larger volume of "healthy" lung tissue is preserved, making the reopening of dorsal atelectatic lung tissue potentially quicker. For non-focal ARDS, a more extended prone positioning time is required for improved oxygenation. This suggests that for this type of patient, a longer prone positioning time is needed to assess the effectiveness of prone positioning.

The varying responses of the prone position to ARDS with different levels of d-dimer may be attributed to the following reasons. D-dimer is a degradation product of fibrin resulting from the fibrinolytic process and is closely associated with thrombosis. As research into immune and coagulation mechanisms advances, it has become clear that inflammation plays a significant role in promoting thrombosis during sepsis, while thrombosis, in turn, exacerbates inflammation [33–35]. More recently, D-dimer has emerged as a potential biomarker for assessing the severity of ARDS, particularly in patients with COVID-19-related ARDS [36–38]. During the progression of ARDS, the interplay between the inflammatory cytokine storm and coagulation dysfunction can lead to pulmonary microthrombosis [39–41]. This pathological process may result in increased dead space and ventilation-perfusion mismatch, which is consistent with the findings observed in our study. Furthermore, elevated D-dimer levels may reflect stronger inflammation and coagulation activity. Under the influence of gravitational compression from surrounding tissues and organs, such as the heart, blood vessels may experience increased microthrombosis. Additionally, the uneven distribution of ventilation and perfusion leads to increased dead space. Therefore, a longer duration of prone positioning is necessary to facilitate the homogenization of changes in both lung ventilation and perfusion.

Our study possesses certain strengths. This is the first study to observe physiological changes after PP in mechanically ventilated ARDS patients with different clinical phenotypes. This study provides a valuable reference for guiding prone position treatment in ARDS patients with diverse clinical phenotypes. However, there are also some limitations. First, this was a single-center, small-sample study, which limits the reliability of our conclusions. Second, D-dimer may be inaccurate as a basis for classifying ARDS subphenotypes. Although D-dimer is a potential marker of inflammation associated with coagulation, there are limited studies on the subphenotype classification of ARDS. Therefore, prospective studies with larger sample sizes are required to further investigate this relationship. There are few studies on the response of patients with different inflammatory subphenotypes of ARDS to clinical treatments. Multiple biomarkers may be needed for joint diagnosis to increase the accuracy of subphenotype diagnosis. Additionally, the observation time in this study was 12 h in the prone position. The inadequate observation time may have led to a lack of relevant data on the effects of longer-duration prone positioning. Finally, the present study employed EIT to monitor lung ventilation-perfusion matching in ARDS patients. This method has spatial limitations and cannot represent the total proportion of ventilation-perfusion matching for all lung tissue.

Conclusion

For moderate to severe ARDS patients, oxygenation, and ventilation-perfusion improve more rapidly after prone positioning in focal or low D-dimer ARDS patients, whereas it takes longer for oxygenation to improve after prone positioning in non-focal and high D-dimer ARDS patients. This recommendation needs validation through a controlled trial with a larger sample size.

Abbreviations

ARDS	Acute respiratory distress syndrome
EIT	Electrical impedance tomography
ICU	Intensive care unite
PBW	Predicted body weight
PP	Prone position
PEEP	Positive end expiratory pressure
SIMV	Synchronized intermittent mandatory ventilation
SP	Supine position
VQ matching	ventilation-perfusion matching
Vt	Tidal volume
RR	Respiratory rate
FiO2	Fraction of inspired oxygen
V/Q	Ventilation/perfusion
GI	Global Inhomogeneity
ROI	Region of Interest

Supplementary Information

The online version contains supplementary material available at https://doi.org/10.1186/s12931-025-03154-4.

Supplementary Material 1

Acknowledgements

The authors thank all the subjects for their participation in this study.

Author contributions

S.Y., Q.S., J.W., and Y.H. conceived the study. S.Y., X.Y., J.X., L.L., and F.G. collected data for the work. S.Y., Q.S., W.H., X.L., and H.W. performed data analysis. S.Y., Q.S., X.L., Q.P., C.Z., W.H., Y.Y., and Y.H. prepared the first draft of the manuscript. All authors were responsible for data interpretation, revised the manuscript critically, and approved the version submitted for publication.

Funding

This study was supported by the National Natural Science Foundation of China (82272235), the Science Foundation of the Commission of Health of Jiangsu Province (ZDB2020009), and the Jiangsu Province Key research and development Program (Social Development) Special Project (BE2021734).

Data availability

No datasets were generated or analysed during the current study.

Declarations

Ethics approval and consent to participate
This study was approved by the local ethics committee(2021ZDSYLL171-P01) and written informed consent was obtained from all participants before enrollment.

Consent for publication
Not applicable.

Competing interests
The authors declare no competing interests.

Author details
[1]Jiangsu Provincial Key Laboratory of Critical Care Medicine, Department of Critical Care Medicine, Zhongda Hospital, School of Medicine, Southeast University, Nanjing 210009, Jiangsu, China

Received: 18 September 2024 / Accepted: 13 February 2025
Published online: 28 February 2025

References

1. Bellani G, Pham T, Laffey J, Investigators L-S, Group ET. Incidence of Acute Respiratory Distress syndrome–reply. JAMA. 2016;316(3):347.
2. Williams GW, Berg NK, Reskallah A, Yuan X, Eltzschig HK. Acute respiratory distress syndrome. Anesthesiology. 2021;134(2):270–82.
3. Piehl MA, Brown RS. Use of extreme position changes in acute respiratory failure. Crit Care Med. 1976;4(1):13–4.
4. Guerin C, Reignier J, Richard JC, Beuret P, Gacouin A, Boulain T, Mercier E, Badet M, Mercat A, Baudin O, et al. Prone positioning in severe acute respiratory distress syndrome. N Engl J Med. 2013;368(23):2159–68.
5. Scholten EL, Beitler JR, Prisk GK, Malhotra A. Treatment of ARDS with Prone Positioning. Chest. 2017;151(1):215–24.
6. Sud S, Friedrich JO, Adhikari NK, Taccone P, Mancebo J, Polli F, Latini R, Pesenti A, Curley MA, Fernandez R, et al. Effect of prone positioning during mechanical ventilation on mortality among patients with acute respiratory distress syndrome: a systematic review and meta-analysis. CMAJ. 2014;186(10):E381–390.
7. Protti A, Santini A, Pennati F, Chiurazzi C, Ferrari M, Iapichino GE, Carenzo L, Dalla Corte F, Lanza E, Martinetti N, et al. Lung response to prone positioning in mechanically-ventilated patients with COVID-19. Crit Care. 2022;26(1):127.
8. Puybasset L, Cluzel P, Gusman P, Grenier P, Preteux F, Rouby JJ. Regional distribution of gas and tissue in acute respiratory distress syndrome. I. consequences for lung morphology. CT scan ARDS Study Group. Intensive Care Med. 2000;26(7):857–69.
9. Gattinoni L, Caironi P, Cressoni M, Chiumello D, Ranieri VM, Quintel M, Russo S, Patroniti N, Cornejo R, Bugedo G. Lung recruitment in patients with the acute respiratory distress syndrome. N Engl J Med. 2006;354(17):1775–86.
10. Jabaudon M, Blondonnet R, Lutz J, Roszyk L, Bouvier D, Guerin R, Perbet S, Cayot S, Godet T, Blanchon L, et al. Net alveolar fluid clearance is associated with lung morphology phenotypes in acute respiratory distress syndrome. Anaesth Crit Care Pain Med. 2016;35(2):81–6.
11. Chen H, Sun Q, Chao Y, Liu Y, Yu Q, Xie J, Pan C, Liu L, Yang Y, Qiu H. Lung morphology impacts the association between ventilatory variables and mortality in patients with acute respiratory distress syndrome. Crit Care. 2023;27(1):59.
12. Calfee CS, Delucchi K, Parsons PE, Thompson BT, Ware LB, Matthay MA, Network NA. Subphenotypes in acute respiratory distress syndrome: latent class analysis of data from two randomised controlled trials. Lancet Respir Med. 2014;2(8):611–20.
13. Gattinoni L, Carlesso E, Taccone P, Polli F, Guerin C, Mancebo J. Prone positioning improves survival in severe ARDS: a pathophysiologic review and individual patient meta-analysis. Minerva Anestesiol. 2010;76(6):448–54.
14. Constantin JM, Jabaudon M, Lefrant JY, Jaber S, Quenot JP, Langeron O, Ferrandiere M, Grelon F, Seguin P, Ichai C, et al. Personalised mechanical ventilation tailored to lung morphology versus low positive end-expiratory pressure for patients with acute respiratory distress syndrome in France (the LIVE study): a multicentre, single-blind, randomised controlled trial. Lancet Respir Med. 2019;7(10):870–80.
15. Force ADT, Ranieri VM, Rubenfeld GD, Thompson BT, Ferguson ND, Caldwell E, Fan E, Camporota L, Slutsky AS. Acute respiratory distress syndrome: the Berlin definition. JAMA. 2012;307(23):2526–33.
16. Brower RG, Lanken PN, MacIntyre N, Matthay MA, Morris A, Ancukiewicz M, Schoenfeld D, Thompson BT, National Heart L, Blood Institute ACTN. Higher versus lower positive end-expiratory pressures in patients with the acute respiratory distress syndrome. N Engl J Med. 2004;351(4):327–36.
17. He H, Chi Y, Long Y, Yuan S, Zhang R, Yang Y, Frerichs I, Moller K, Fu F, Zhao Z. Three broad classifications of acute respiratory failure etiologies based on regional ventilation and perfusion by electrical impedance tomography: a hypothesis-generating study. Ann Intensive Care. 2021;11(1):134.
18. Zhao Z, Moller K, Steinmann D, Frerichs I, Guttmann J. Evaluation of an electrical impedance tomography-based Global Inhomogeneity Index for pulmonary ventilation distribution. Intensive Care Med. 2009;35(11):1900–6.
19. Spinelli E, Kircher M, Stender B, Ottaviani I, Basile MC, Marongiu I, Colussi G, Grasselli G, Pesenti A, Mauri T. Unmatched ventilation and perfusion measured by electrical impedance tomography predicts the outcome of ARDS. Crit Care. 2021;25(1):192.
20. Austin JH, Muller NL, Friedman PJ, Hansell DM, Naidich DP, Remy-Jardin M, Webb WR, Zerhouni EA. Glossary of terms for CT of the lungs: recommendations of the Nomenclature Committee of the Fleischner Society. Radiology. 1996;200(2):327–31.
21. Musso G, Taliano C, Molinaro F, Fonti C, Veliaj D, Torti D, Paschetta E, Castagna E, Carbone G, Laudari L, et al. Early prolonged prone position in noninvasively ventilated patients with SARS-CoV-2-related moderate-to-severe hypoxemic respiratory failure: clinical outcomes and mechanisms for treatment response in the PRO-NIV study. Crit Care. 2022;26(1):118.
22. Wang YX, Zhong M, Dong MH, Song JQ, Zheng YJ, Wu W, Tao JL, Zhu L, Zheng X. Prone positioning improves ventilation-perfusion matching assessed by electrical impedance tomography in patients with ARDS: a prospective physiological study. Crit Care. 2022;26(1):154.
23. Mauri T, Bellani G, Confalonieri A, Tagliabue P, Turella M, Coppadoro A, Citerio G, Patroniti N, Pesenti A. Topographic distribution of tidal ventilation in acute respiratory distress syndrome: effects of positive end-expiratory pressure and pressure support. Crit Care Med. 2013;41(7):1664–73.
24. Galiatsou E, Kostanti E, Svarna E, Kitsakos A, Koulouras V, Efremidis SC, Nakos G. Prone position augments recruitment and prevents alveolar overinflation in acute lung injury. Am J Respir Crit Care Med. 2006;174(2):187–97.
25. Lamm WJ, Graham MM, Albert RK. Mechanism by which the prone position improves oxygenation in acute lung injury. Am J Respir Crit Care Med. 1994;150(1):184–93.
26. Musch G, Layfield JD, Harris RS, Melo MF, Winkler T, Callahan RJ, Fischman AJ, Venegas JG. Topographical distribution of pulmonary perfusion and ventilation, assessed by PET in supine and prone humans. J Appl Physiol (1985). 2002;93(5):1841–51.
27. Perier F, Tuffet S, Maraffi T, Alcala G, Victor M, Haudebourg AF, De Prost N, Amato M, Carteaux G, Mekontso Dessap A. Effect of positive end-expiratory pressure and proning on Ventilation and Perfusion in COVID-19 Acute Respiratory Distress Syndrome. Am J Respir Crit Care Med. 2020;202(12):1713–7.
28. Glenny RW, Lamm WJ, Albert RK, Robertson HT. Gravity is a minor determinant of pulmonary blood flow distribution. J Appl Physiol (1985). 1991;71(2):620–9.
29. Fossali T, Pavlovsky B, Ottolina D, Colombo R, Basile MC, Castelli A, Rech R, Borghi B, Ianniello A, Flor N, et al. Effects of Prone position on lung recruitment and ventilation-perfusion matching in patients with COVID-19 Acute Respiratory Distress Syndrome: A Combined CT Scan/Electrical Impedance Tomography Study. Crit Care Med. 2022;50(5):723–32.
30. Yuan X, Zhao Z, Chao Y, Chen D, Chen H, Zhang R, Liu S, Xie J, Yang Y, Qiu H, et al. Effects of early versus delayed application of prone position on ventilation-perfusion mismatch in patients with acute respiratory distress syndrome: a prospective observational study. Crit Care. 2023;27(1):462.
31. Pelosi P, D'Andrea L, Vitale G, Pesenti A, Gattinoni L. Vertical gradient of regional lung inflation in adult respiratory distress syndrome. Am J Respir Crit Care Med. 1994;149(1):8–13.
32. Gattinoni L, Pesenti A, Carlesso E. Body position changes redistribute lung computed-tomographic density in patients with acute respiratory failure: impact and clinical fallout through the following 20 years. Intensive Care Med. 2013;39(11):1909–15.
33. Jackson SP, Darbousset R, Schoenwaelder SM. Thromboinflammation: challenges of therapeutically targeting coagulation and other host defense mechanisms. Blood. 2019;133(9):906–18.

34. Delabranche X, Helms J, Meziani F. Immunohaemostasis: a new view on haemostasis during sepsis. Ann Intensive Care. 2017;7(1):117.
35. Engelmann B, Massberg S. Thrombosis as an intravascular effector of innate immunity. Nat Rev Immunol. 2013;13(1):34–45.
36. Ponti G, Maccaferri M, Ruini C, Tomasi A, Ozben T. Biomarkers associated with COVID-19 disease progression. Crit Rev Clin Lab Sci. 2020;57(6):389–99.
37. Wu C, Chen X, Cai Y, Xia J, Zhou X, Xu S, Huang H, Zhang L, Zhou X, Du C, et al. Risk factors Associated with Acute respiratory distress syndrome and death in patients with Coronavirus Disease 2019 Pneumonia in Wuhan, China. JAMA Intern Med. 2020;180(7):934–43.
38. Fuchs-Buder T, de Moerloose P, Ricou B, Reber G, Vifian C, Nicod L, Romand JA, Suter PM. Time course of procoagulant activity and D dimer in bronchoalveolar fluid of patients at risk for or with acute respiratory distress syndrome. Am J Respir Crit Care Med. 1996;153(1):163–7.
39. Bansal A, Singh AD, Jain V, Aggarwal M, Gupta S, Padappayil RP, Nadeem M, Joshi S, Mian A, Greathouse T, et al. The association of D-dimers with mortality, intensive care unit admission or acute respiratory distress syndrome in patients hospitalized with coronavirus disease 2019 (COVID-19): a systematic review and meta-analysis. Heart Lung. 2021;50(1):9–12.
40. Estenssoro E, Loudet CI, Dubin A, Kanoore Edul VS, Plotnikow G, Andrian M, Romero I, Sagardia J, Bezzi M, Mandich V, et al. Clinical characteristics, respiratory management, and determinants of oxygenation in COVID-19 ARDS: a prospective cohort study. J Crit Care. 2022;71:154021.
41. Iba T, Levy JH, Levi M, Connors JM, Thachil J. Coagulopathy of Coronavirus Disease 2019. Crit Care Med. 2020;48(9):1358–64.

Publisher's note

Springer Nature remains neutral with regard to jurisdictional claims in published maps and institutional affiliations.